Thermal Conductivity of $Ho_2Ti_2O_7$ along the [111] Direction

W. H. Toews,[1,2] Songtian S. Zhang,[2] K. A. Ross,[3] H. A. Dabkowska,[3,4] B. D. Gaulin,[3,4,5] and R. W. Hill[1,2]

[1]*Guelph-Waterloo Physics Institute, University of Waterloo, Waterloo, Ontario N2L 3G1, Canada*
[2]*Department of Physics and Astronomy, University of Waterloo, Waterloo, Ontario N2L 3G1, Canada*
[3]*Department of Physics and Astronomy, McMaster University, Hamilton, Ontario L8S 4M1, Canada*
[4]*Brockhouse Institute for Materials Research, McMaster University, Hamilton, Ontario L8S 4M1, Canada*
[5]*Canadian Institute for Advanced Research, 180 Dundas Street West, Toronto, Ontario, M5G 1Z8, Canada*

(Received 17 August 2012; revised manuscript received 15 April 2013; published 23 May 2013)

Thermal transport measurements have been made on the spin-ice material $Ho_2Ti_2O_7$ in an applied magnetic field with both the heat current and the field parallel to the [111] direction for temperatures from 50 mK to 1.2 K. A large magnetic field >6 T is applied to suppress the magnetic contribution to the thermal conductivity in order to extract the lattice conductivity. The low field thermal conductivity thus reveals a magnetic field dependent contribution to the conductivity which both transfers heat and scatters phonons. We interpret these magnetic excitations as monopolelike excitations and describe their behavior via existing Debye-Hückel theory.

DOI: 10.1103/PhysRevLett.110.217209 PACS numbers: 75.25.−j, 14.80.Hv, 66.70.−f, 75.47.−m

The search for isolated magnetic monopoles as elementary particles has captivated physicists since Dirac's seminal work of the 1930s. The most recent chapter in this area involves the idea of monopoles as emergent particles manifested in the collective behavior of a large number of interacting spins. Such exotic physics has recently been theoretically proposed to exist in frustrated magnetic systems known as spin ice [1].

One example of a spin-ice material is $Ho_2Ti_2O_7$ (HTO), a rare-earth titanate which crystallizes in the pyrochlore structure, which puts the spins due to the Ho^{3+} ions on the vertices of a lattice of corner-sharing tetrahedra. The ground state is a nearly perfect Ising system such that the large magnetic moment $\mu = 10\mu_B$ is quantized along the local [111] direction (into or out of each tetrahedron) [2]. The effective magnetic interaction between these spins is ferromagnetic with a remarkable consequence for the ground state, which is macroscopically degenerate with the spins arranged so that two spins point into each tetrahedron and two spins point out of each tetrahedron (i.e., there is a sixfold degeneracy for each tetrahedron) [2]. The name spin ice derives from the degeneracy of the ground state, which gives rise to a residual entropy of $S = (k_B/2)\ln(3/2)$ per spin and is well approximated by the Pauling entropy in water ice resulting from proton disorder [3].

Excitations out of the 2-in-2-out ground state are theoretically proposed to be analogous to "magnetic monopole–like" quasiparticles. The reasoning is that a single spin flip will create a tetrahedron with 3 spins in and 1 out (monopole) and a tetrahedron with 1 spin in and 3 out (antimonopole) as a consequence of the corner-sharing tetrahedra. Once this initial energy barrier is overcome, subsequent spin flips required to separate the monopole-antimonopole pair do not further violate the 2-in-2-out ice rules and thus they behave as "free" particles interacting with a Coulomb interaction [1].

Experimentally, the spin-ice ground state in HTO and in isostructural $Dy_2Ti_2O_7$ (DTO) has been established through measurements of the specific heat, which when integrated lead to a residual ground state entropy that is in close agreement with the Pauling value [4–8].

Conversely, measurements attempting to observe magnetricity, a magnetic monopole current in spin ice, are less definitive. Initial muon spin rotation measurements of DTO [9], which mapped the monopole current onto Onsager's theory of electrolytes, are now the subject of debate over exactly where the muon signal originates [10,11]. Moreover, measurements of the electromotive force induced in a solenoid from a relaxing magnetic current [12] infer magnetic relaxation times that are not observed in more recent magnetic susceptibility measurements [13].

In this Letter, we present thermal conductivity measurements of HTO in the very low temperature range with a magnetic field along the [111] crystallographic direction. Our goal is to shed light on the properties of the magnetic excitations and to see to what extent they can be described by a theory of magnetic monopoles. Thermal conductivity is an excellent tool for probing the behavior of delocalized quasiparticles in materials, for example, superconducting quasiparticles [14] or magnons [15]. In spin-ice materials, similar experiments have been conducted in DTO [16,17]. However, in these works, the magnetic excitations were assumed to be either localized and only affect the thermal conductivity through their interaction with phonons [16], or delocalized and conduct heat but have no affect on the phonon conductivity [17]. Our results provide clear evidence that the magnetic excitations act both as a channel for heat transport and as a strong scattering mechanism for

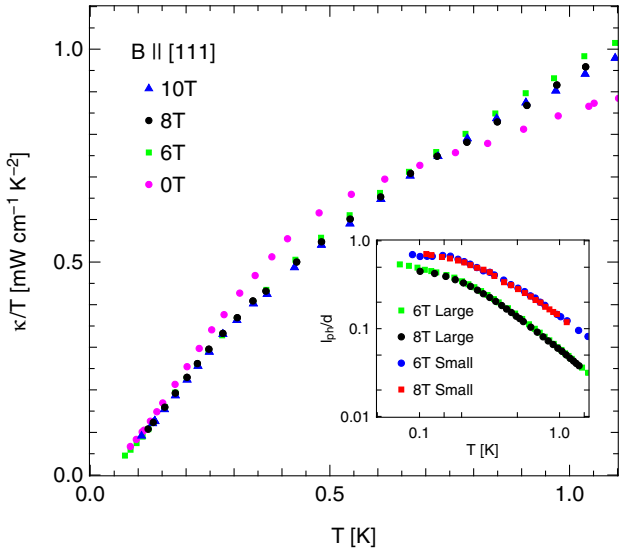

FIG. 1 (color online). Thermal conductivity divided by temperature is plotted versus temperature for the large HTO sample with heat current along the [111] direction in magnetic fields of $B = 0$, 6, 8, 10 T applied parallel to [111]. Inset: The temperature dependence of the phonon mean free path l_{ph} divided by sample width d for the large and small samples at 6 and 8 T.

phonons. We also find that the temperature dependence of the heat transport and scattering rate are consistent with current theoretical models that describe the magnetic excitations as monopoles.

A large single crystal of HTO was grown using the floating-zone image method [18]. From this, we prepared two thin rectangular prisms with dimensions $0.34 \times 0.35 \times 2.0$ mm^3 (large sample) and $0.10 \times 0.17 \times 0.35$ mm^3 (small sample) with the [111] axis parallel to the long axis. Samples of different dimension are measured to help rigorously identify the phonon conductivity as we show below. Thermal conductivity (κ) was measured via the one-heater–two-thermometer method [19] with the heat current and applied magnetic field (B) parallel to the [111] axis for temperatures from $T = 50$ mK to 1.2 K. Quasistatic temperature sweeps were conducted in a variety of applied magnetic fields between the spin-ice state at 0 T, the plateau "kagome-ice" state at approximately 0.5 T and in the 3-in-1-out or 1-in-3-out state at 6, 8, and 10 T. For each sweep, the resistive thermometers were calibrated *in situ* against the dilution fridge temperature. These materials are known to exhibit long time constants at low temperature [20]. Extreme care was taken to ensure the sample was thermally equilibrated with the fridge at each temperature step by waiting for up to 1.5×10^4 s at the lowest temperatures before measuring. Thermal conductivity was measured at 190 mK for 24 h, which showed no sign of evolution beyond 1.5×10^4 s, thus ensuring our settling time was adequate. The magnetic field was applied at sample temperatures above 1.5 K and the samples subsequently field cooled to perform temperature sweeps. The absolute error in the conductivity values is dominated by an uncertainty of ~10% in the geometric factor in the large sample and ~20% in the smaller sample. The relative uncertainty between each data set is less than 1%, as illustrated by the error bar in Fig. 2.

Figure 1 presents κ/T versus T for the large sample in applied magnetic fields of 0 T and 6, 8, and 10 T. The in-field data at 6, 8, and 10 T are all identical within experimental error below $T = 0.8$ K. Above this temperature, the 6 T data are systematically higher at the few percent level. The 0 T data show an increase in conductivity over the in-field data for $T < 0.65$ K. Above $T = 0.65$ K, the zero field conductivity is suppressed below the in-field data which indicates the presence of an additional scattering mechanism. Identical qualitative features are also observed in the small sample. However, the conductivity grows less rapidly at the lowest temperatures (see inset of Fig. 3), which, as we discuss below, is consistent with the smaller sample dimensions.

In a magnetic insulator, the thermal conductivity has two contributions: the lattice (phonons) and magnetic excitations. In order to observe the effect of magnetic excitations on the thermal conductivity, either as a phonon scattering mechanism or as a conductivity channel itself, the phonon conductivity must be established in the absence of any magnetic excitations. This is often achieved via measuring a nonmagnetic, isostructural material. However, in this case we obtain the phonon conductivity by using a large magnetic field to drive the system into a magnetically ordered state where magnetic excitations are strongly suppressed. This technique has been successfully used in other magnetic systems [21]. In HTO, a field of 2.5 T along the [111] direction is sufficient to break the 2-in-2-out ice rules, resulting in a 3-in-1-out or 1-in-3-out state where the magnetization becomes constant with magnetic field [22]. This is consistent with our observation that the temperature dependence of the thermal conductivity is constant for magnetic fields from 6 to 10 T. As a result, we consider the 6, 8, and 10 T thermal conductivity to be entirely due to phonons. Conversely, the zero field conductivity includes magnetic contributions to both conduction and scattering.

Further analysis of the phonon conductivity is done by examining the phonon mean free path l_{ph}. This can be extracted from the phonon thermal conductivity (κ_{ph}) via kinetic theory:

$$l_{\mathrm{ph}} = 3\frac{\kappa_{\mathrm{ph}}}{c_{\mathrm{ph}} v_s}, \tag{1}$$

where $c_{\mathrm{ph}} = 4.8T^3 \times 10^{-4}$ J K^{-1} mol^{-1} [8] is the phonon specific heat, $v_s = 3.2 \times 10^3$ ms^{-1} [23] is the speed of sound, and $\kappa_{\mathrm{ph}} = \kappa_{\mathrm{total}}(8\ \mathrm{T})$ (choosing the 8 T data set as representative of the in-field data). The mean free path, l_{ph}, normalized by the geometric average of the sample width, $d = \sqrt{4A/\pi} = 0.41(0.15)$ mm for the large (small) sample, is plotted versus temperature in the inset of Fig. 1, where A is the sample cross-sectional area. As the

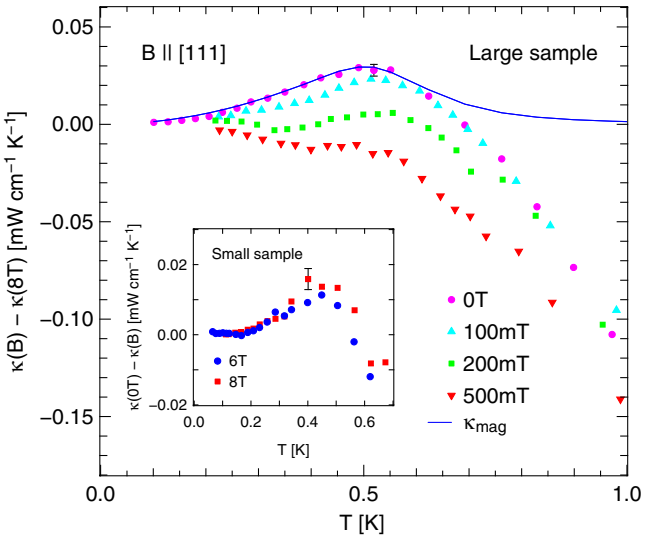

FIG. 2 (color online). Difference between thermal conductivity at 8 T, $\kappa(8\ \mathrm{T})$, and the low field conductivity, $\kappa(B)$, for the large sample with $B = 0$, 0.1, 0.2, 0.5 T. The magnetic contribution to the conductivity obtained from fitting is also included (solid blue line). Inset: Difference between the 0 T conductivity and high field conductivities with $B = 8$ T and $B = 6$ T for the small sample.

temperature approaches $T = 0$, the phonon scattering becomes temperature independent and the mean free path approaches a value close to the sample dimensions (Casimir limit). In the smaller sample, the boundary limit is achieved at a higher temperature (~ 200 mK) consistent with the shorter mean free path.

As the temperature is increased, the reduction of the phonon mean free path from the boundary limited value indicates the presence of additional temperature dependent scattering mechanisms. This is described using kinetic theory and Matthiessen's rule:

$$\kappa_{\mathrm{ph}} = \kappa_{\mathrm{total}}(8\ \mathrm{T}) = \frac{1}{3}\frac{c_{\mathrm{ph}} v_s^2}{\sum_i \Gamma_i}, \tag{2}$$

where Γ_i are the scattering rates from different nonmagnetic mechanisms. These scattering mechanisms may include the sample boundaries ($\Gamma_B \sim v_s/d$), dislocations ($\Gamma_D \sim T$), and point defects ($\Gamma_{\mathrm{PD}} \sim T^4$) [24]. In order to fit the phonon conductivity, the functional forms of the dislocation and point defect scattering terms are exact and the coefficients are left as fitting parameters. These fitting parameters are expected to be sample independent since they are cut from the same single crystal. Conversely, the coefficient of the boundary scattering term is determined by the sample dimensions (and the phonon specific heat and the speed of sound) through Eq. (1). The simplest functional form of the conductivity due to boundary scattering is proportional to T^3 with the temperature dependence coming entirely from the phonon specific heat, Eq. (2). However, a more realistic functional form has an exponent slightly below 3 due to the effects on thermal conductivity from specular and diffuse boundary scattering, as has been examined in depth in other insulating materials [15,25–27]. The results of this analysis using one set of parameters are shown for both samples in the inset of Fig. 3. The best fit is achieved for a boundary scattering conductivity displaying a $T^{2.85}$ temperature dependence in addition to dislocation and point defect terms [28]. Despite its simplicity, this model for the phonon conductivity clearly shows the dominance of boundary scattering at the very lowest temperatures including the correct scaling with sample size. At higher temperatures (>0.2 K), the scattering is dominated by temperature dependent terms, which we model as point defects and dislocations and are the same for both samples. Although the exact origin is unknown, such terms are consistent with recent Monte Carlo modeling of magnetic susceptibility measurements in DTO, which inferred 0.03% stuffing (excess magnetic Dy ions on Ti sites) [29]. Such interion substitution would undoubtedly have an impact on phonon transport.

Turning now to the magnetic excitations, Fig. 2 shows the zero field and other low field runs less the 8 T data for the large sample. This illuminates the magnetic field dependence of the increased conductivity at low temperatures ($T \lesssim 0.65$ K) followed by the large decrease in conductivity as temperature increases, with respect to $\kappa_{\mathrm{ph}} = \kappa_{\mathrm{total}}(8\ \mathrm{T})$. Within the magnetic monopole picture, the source of additional magnetic conductivity at low temperature is delocalized magnetic monopole excitations. At the lowest temperatures the density of monopoles is sufficiently low that they do not cause scattering. As the temperature is increased, the density increases rapidly and they strongly scatter each other and the phonons, resulting in the suppressed conductivity. Furthermore, the increased (magnetic) conductivity below 0.65 K is suppressed by an applied magnetic field. Qualitatively, a possible explanation of this is as follows. From the perspective of the [111] direction, the corner-shared tetrahedra on which the Ho^{3+} ions reside can be viewed as a stack of alternating kagome and triangular planes. Introducing an externally applied magnetic field along the [111] direction will polarize the spins in the triangular lattice and effectively decouple the intervening kagome planes yet retain the 2-in-2-out ground state. This is known as the kagome-ice state [22]. In this state, magnetic excitations are confined to the kagome planes which are perpendicular to the direction of heat flow and thus do not contribute to the conductivity. However, these excitations will continue to scatter the phonons, and hence the decrease in conductivity above $T \sim 0.65$ K remains. The inset of Fig. 2 shows the difference between the 0 T data and the high field (6 and 8 T) data for the small sample. The qualitative temperature dependence is the same as for the large sample. However, the magnitude of the magnetic contribution of the small sample is less than that of the large sample, which is not understood.

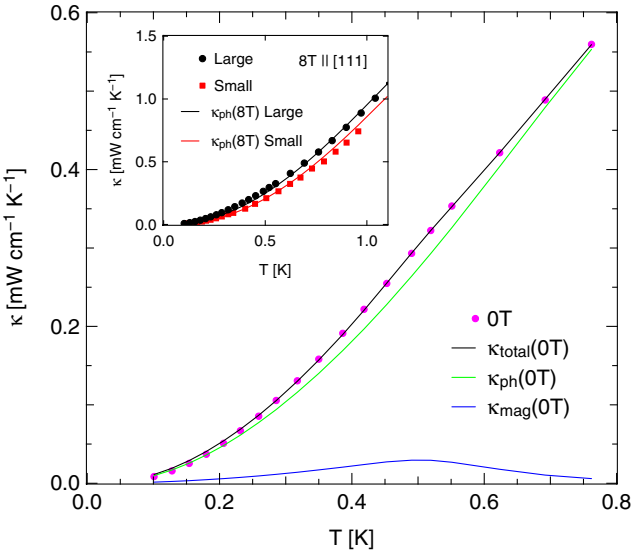

FIG. 3 (color online). Total zero field thermal conductivity for the large sample (pink circles) fitted to Eq. (4) (black line) such that $\kappa_{\rm mag} = T^2[A_1 + A_2\rho(T)]^{-1}$ and $\Gamma_{\rm mag} \propto \rho(T)$. The individual components to the conductivity, $\kappa_{\rm mag}$ (blue line) and $\kappa_{\rm ph}$ (green line), are also represented. Inset: Thermal conductivity in an applied field of 8 T for the large (black circles) and small (red squares) samples. These data are fitted using kinetic theory described in Eq. (2) (solid lines).

The low field thermal conductivity clearly shows that the magnetic excitations conduct heat and provide a scattering mechanism. Therefore, analysis of the 0 T data must include a magnetic contribution to the conductivity $\kappa_{\rm mag}$ (in addition to $\kappa_{\rm ph}$) and also a magnetic contribution to the phonon scattering $\Gamma_{\rm mag}$. Thus, $\kappa_{\rm total}(0\ {\rm T})$ can be written using Matthiessen's rule as

$$\kappa_{\rm total}(0\ {\rm T}) = \kappa_{\rm mag} + \frac{1}{3}\frac{c_{\rm ph}v_s^2}{\Gamma_{\rm mag} + \sum_i \Gamma_i} = \kappa_{\rm mag} + \left(\frac{3}{c_{\rm ph}v_s^2}\Gamma_{\rm mag} + \frac{1}{\kappa_{\rm total}(8\ {\rm T})}\right)^{-1}. \quad (3)$$

The functional form of the magnetic contribution to the conductivity $\kappa_{\rm mag}$ is unknown. However, assuming that the main scattering mechanism at the lowest temperatures is due to point defects and is therefore temperature independent, we use the form expected for massive excitations in three dimensions such that $\kappa_{\rm mag} \sim T^2$ [30]. As the temperature increases, we assume that the monopoles interact with each other such that their scattering rate is proportional to the monopole density $\rho(T)$. Thus, the total magnetic contribution to the thermal conductivity can be written as $\kappa_{\rm mag} = T^2[A_1 + A_2\rho(T)]^{-1}$, where A_1 and A_2 are fitting parameters. As shown in Fig. 2, this simple model provides an excellent fit to the data at low temperatures where the density of monopoles is low, the scattering of phonons is small, and the subtraction accurately reflects the magnetic contribution alone. Beyond the peak, the number of monopoles proliferates and the scattering affects both the magnetic and phonon conductivity so the subtracted data include the suppression of both phonons as well as the monopole current.

As a first approximation, the magnetic-phonon scattering rate is assumed to be proportional to the monopole density, $\Gamma_{\rm mag} \propto \rho(T)$. The monopole density can be determined from the dressed energy Δ_d required to create an isolated monopole using Debye-Hückel theory [31]:

$$\rho(T) \propto \frac{2e^{-\Delta_d/T}}{1 + 2e^{-\Delta_d/T}} \sim e^{-\Delta_d/T}\ (T \to 0\ {\rm K}). \quad (4)$$

Using the dressed energy for monopole creation accounts for the reduction in the bare energy, $\Delta = 5.8$ K [31], of creating an isolated monopole due to the screening effect of any surrounding monopoles on the Coulomb interaction between a monopole-antimonopole pair. The dressed and bare energies are related by

$$\Delta_d = \Delta - \frac{E_{\rm nn}}{2}\frac{a_d}{\xi_{\rm Debye}}, \quad (5)$$

where the screening length $\xi_{\rm Debye}$ is determined in turn by the monopole density

$$\frac{\xi_{\rm Debye}}{a_d} = \sqrt{\frac{2}{3\sqrt{3}\pi E_{\rm nn}}}\sqrt{\frac{T}{\rho(T)}}. \quad (6)$$

Here, $a_d = 4.34$ Å is the distance between the centers of neighboring tetrahedra (i.e., the nearest neighbor distance between monopoles) and $E_{\rm nn} = 3.06$ K is the Coulomb energy of two monopoles on neighboring sites. There is no analytical solution to Eqs. (4) and (6) which must be solved self-consistently.

To access the monopole-phonon scattering, we fit the full zero field data to Eqs. (3) and (6). For the large sample, the result is seen in Fig. 3 along with the individual components to the conductivity, $\kappa_{\rm mag}$ and $\kappa_{\rm ph}$. From a qualitative standpoint, the description of the temperature dependence is excellent. This indicates that not only is the additional transport provided by the magnetic excitations well described by our model, but also the monopole-phonon scattering is proportional to the temperature dependence of the monopole density. Quantitatively, the only fitting parameters are the coefficients of the T^2 term in $\kappa_{\rm mag}$ and the coefficient of the $\rho(T)$ term in $\Gamma_{\rm mag}$ [32]. The monopole-phonon scattering rate obtained from our fit at $T = 500$ mK is approximately 10^8 s^{-1}, which is the same order of magnitude reported for the magnetic scattering of phonons (τ_γ) in DTO [16]. Moreover, the magnitude of $\kappa_{\rm mag}$ can be assessed using kinetic theory. Following Kolland *et al.* [17], a monopole velocity of ~20 m/s (generated from an effective bandwidth for monopole hopping ~1 K and a hopping distance a_d) is assumed. We also take the measured magnetic specific heat for DTO as 256.4 J/K m^3 at 400 mK [33]. Then, using our value for $\kappa_{\rm mag} \sim 2.2 \times 10^{-3}$ W/K m for the large sample

at 400 mK, we obtain a mean free path, $l_{\mathrm{mp}} \sim 1.3\ \mu$m. This is likely an upper bound on l_{mp} given that the magnetic specific heat may well be much smaller in HTO, but the presence of the Schottky anomaly makes obtaining a definite value more difficult [5]. A more important issue is whether the kinetic theory really makes sense. For instance, the monopole velocity could equally be estimated from the Monte Carlo time step, 0.26 ms at 700 mK [29], or from a hopping frequency, $1.8 \times 10^3\ \mathrm{s}^{-1}$, taken from magnetic relaxation experiments [12]. In both cases, this leads to a velocity $\sim 10^6$ times smaller than estimated from the hopping bandwidth and a mean free path of order meters, which is many orders of magnitude larger than the sample. Clearly, further theoretical work will be required to see how to make sense of the magnitude of the conductivity. We do not expect a contribution from collective magnetic excitations such as loop flips described by Melko and Gingras [4] as they are not experimentally accessible at these temperatures due to a large energy barrier.

In conclusion, we have shown that the magnetic excitations of the spin-ice ground state of $Ho_2Ti_2O_7$ give rise to an additional channel for thermal conduction and also prove to be an effective phonon scattering mechanism. We have also shown that the magnetic conductivity channel is consistent with monopoles scattering from point defects and each other. Similarly, the magnetic phonon scattering rate is proportional to the monopole density, as determined by Debye-Hückel theory. This provides strong evidence that these excitations can be thought of as delocalized, magnetic monopolelike quasiparticles.

This research was supported by NSERC of Canada. We would also like to thank A. L. Chernyshev, D. G. Hawthorn, P. Henelius, J. B. Kycia, and R. G. Melko for thought-provoking conversations.

[1] C. Castelnovo, R. Moessner, and S. Sondhi, Nature (London) **451**, 42 (2008).
[2] S. T. Bramwell and M. Gingras, Science **294**, 1495 (2001).
[3] L. Pauling, J. Am. Chem. Soc. **57**, 2680 (1935).
[4] R. Melko and M. Gingras, J. Phys. Condens. Matter **16**, R1277 (2004).
[5] S. T. Bramwell, M. J. Harris, B. C. den Hertog, M. J. P. Gingras, J. S. Gardner, D. F. McMorrow, A. R. Wildes, A. L. Cornelius, J. D. M. Champion, R. G. Melko, and T. Fennell, Phys. Rev. Lett. **87**, 047205 (2001).
[6] R. Higashinaka, H. Fukazawa, and Y. Maeno, Phys. Rev. B **68**, 014415 (2003).
[7] R. Higashinaka, H. Fukazawa, K. Deguchi, and Y. Maeno, J. Phys. Condens. Matter **16**, S679 (2004).
[8] Z. Hiroi, K. Matsuhira, S. Takagi, T. Tayama, and T. Sakakibara, J. Phys. Soc. Jpn. **72**, 2 (2003).
[9] S. T. Bramwell, S. R. Giblin, S. Calder, R. Aldus, D. Prabhakaran, and T. Fennell, Nature (London) **461**, 956 (2009).
[10] S. R. Dunsiger, A. A. Aczel, C. Arguello, H. Dabkowska, A. Dabkowski, M. H. Du, T. Goko, B. Javanparast, T. Lin, F. L. Ning, H. M. L. Noad, D. J. Singh, T. J. Williams, Y. J. Uemura, M. J. P. Gingras, and G. M. Luke, Phys. Rev. Lett. **107**, 207207 (2011).
[11] S. J. Blundell, Phys. Rev. Lett. **108**, 147601 (2012).
[12] S. R. Giblin, S. T. Bramwell, P. C. Holdsworth, D. Prabhakaran, and I. Terry, Nat. Phys. **7**, 252 (2011).
[13] L. R. Yaraskavitch, H. M. Revell, S. Meng, K. A. Ross, H. M. L. Noad, H. A. Dabkowska, B. D. Gaulin, and J. B. Kycia, Phys. Rev. B **85**, 020410(R) (2012).
[14] M. Sutherland, J. Dunn, W. H. Toews, E. O'Farrell, J. Analytis, I. Fisher, and R. W. Hill, Phys. Rev. B **85**, 014517 (2012).
[15] S. Y. Li, J.-B. Bonnemaison, A. Payeur, P. Fournier, C. H. Wang, X. H. Chen, and L. Taillefer, Phys. Rev. B **77**, 134501 (2008).
[16] B. Klemke, M. Meissner, P. Strehlow, K. Kiefer, S. A. Grigera, and D. A. Tennant, J. Low Temp. Phys. **163**, 345 (2011).
[17] G. Kolland, O. Breunig, M. Valldor, M. Hiertz, J. Frielingsdorf, and T. Lorenz, Phys. Rev. B **86**, 060402 (R) (2012).
[18] J. P. Clancy, J. P. C. Ruff, S. R. Dunsiger, Y. Zhao, H. A. Dabkowska, J. S. Gardner, Y. Qiu, J. R. D. Copley, T. Jenkins, and B. D. Gaulin, Phys. Rev. B **79**, 014408 (2009).
[19] W. H. Toews, Master's thesis, University of Waterloo, 2012.
[20] O. A. Petrenko, M. R. Lees, and G. Balakrishnan, J. Phys. Condens. Matter **23**, 164218 (2011).
[21] Z. Y. Zhau, X. M. Wang, C. Fan, W. Tao, X. G. Liu, W. P. Ke, F. B. Zhang, X. Zhao, and X. F. Sun, Phys. Rev. B **83**, 014414 (2011).
[22] K. Matsuhira, Z. Hiroi, T. Tayama, S. Takagi, and T. Sakakibara, J. Phys. Condens. Matter **14**, L559 (2002).
[23] Y. Nakanishi, T. Kumagai, M. Yoshizawa, K. Matsuhira, S. Takagi, and Z. Hiroi, Phys. Rev. B **83**, 184434 (2011).
[24] R. Berman, *Thermal Conduction In Solids* (Clarendon, Oxford, 1976).
[25] X. F. Sun and Y. Ando, Phys. Rev. B **79**, 176501 (2009).
[26] R. O. Pohl and B. Stritzer, Phys. Rev. B **25**, 3608 (1982).
[27] P. D. Thacher, Phys. Rev. **156**, 975 (1967).
[28] The phonon scattering rates from dislocations and point defects obtained from fitting the 8 T conductivity are $\Gamma_D = 1.1 \times 10^7 T\ \mathrm{s}^{-1}$ and $\Gamma_{\mathrm{PD}} = 1.3 \times 10^6 T^4\ \mathrm{s}^{-1}$, respectively.
[29] H. M. Revell, L. R. Yaraskavitch, J. D. Mason, K. A. Ross, H. M. L. Noad, H. A. Dabkowska, B. D. Gaulin, P. Henelius, and J. B. Kycia, Nat. Phys. **9**, 34 (2012).
[30] Y. Kohama, A. V. Sologubenko, N. R. Dilley, V. S. Zapf, M. Jaime, J. A. Mydosh, A. Paduan-Filho, K. A. Al-Hassanieh, P. Sengupta, S. Gangadharaiah, A. L. Chernyshev, and C. D. Batista, Phys. Rev. Lett. **106**, 037203 (2011).
[31] C. Castelnovo, R. Moessner, and S. L. Sondhi, Phys. Rev. B **84**, 144435 (2011).
[32] The coefficients obtained from fitting the 0 T conductivity are $\kappa_{\mathrm{mag}} = T^2[7.2 + 1.4 \times 10^5 \rho(T)]^{-1}$ and $\Gamma_{\mathrm{mag}} = 1.2 \times 10^8 \rho(T)$.
[33] D. J. P. Morris, D. A. Tennant, S. A. Grigera, B. Klemke, C. Castelnovo, R. Moessner, C. Czternasty, M. Meissner, K. C. Rule, J. U. Hoffmann, K. Kiefer, S. Gerischer, D. Slobinsky, and R. S. Perry, Science **326**, 411 (2009).